HETEROCYCLES, Vol. 70, 2006, pp. 345 - 354. © The Japan Institute of Heterocyclic Chemistry
Received, 31st August, 2006, Accepted, 5th October, 2006, Published online, 6th October, 2006. COM-06-S(W)32

DUAL FLUORESCENCE SPECTRA OF 1-HYDROXYINDOLES WITH VARIOUS C-C-N_b SIDE CHAINS AT 3-POSITION IN METHANOL[#]

Kunihiro Tokumura*, Akio Hayashi, Kenta Imai, and Masanori Somei*

Division of Pharmaceutical Sciences, Graduate School of Natural Science and Technology, Kanazawa University, Kakuma-machi, Kanazawa, 920-1192, Japan
e-mail address: tokumura@kenroku.kanazawa-u.ac.jp

Abstract – Almost the same ultraviolet absorption spectra with a broad peak at 292-294 nm and a shoulder peak at 275 nm were observed for methanol solutions of 1-hydroxyindoles with various C-C-N_b side chains at 3-position such as 1-hydroxy-*N*$_b$-methoxycarbonyltryptamine (1), *N*$_b$-acetyl-1-hydroxytryptophan methyl ester (2), *N*, *N*-dimethyl-1-hydroxyindole-3-acetamide (3), and 1-hydroxy-*N*$_b$-pivaloyltryptamine (4). Dual fluorescence excitation and emission spectra resulting from $^1L_a \rightarrow {}^1A$ and $^1L_b \rightarrow {}^1A$ fluorescence emissions were observed for these 1-hydroxyindoles (1 – 4). Excitation spectra were found to be dependent on observing wavelength of broad fluorescence emission spectra (λ_{max} = 346-350 nm for 1, 2, and 3; λ_{max} = 366 nm for 4). Dual fluorescence behaviors can be explained by the fact that ^1L_a state locates slight below ^1L_b state, and it is supported by time-dependent density functional theory calculations of 1 – 4 in methanol. It is noteworthy that dual fluorescence behaviors are delicately modified by C-C-N_b side chain at 3-position of indole ring.

INTRODUCTION

In the metabolism and biosyntheses of living cells, 1-hydroxytryptophan derivatives should be regarded as a key compound undergoing nucleophilic substitution reactions to generate bioactive 5-hydroxyindole derivatives such as serotonin, melatonin, and bufotenin.[1] It is therefore implied that various bioactive compounds and drugs may be formed *in vitro* from 1-hydroxyindoles including 1-hydroxytryptophans.[1] Preparation of 1-hydroxyindoles is very meaningful in this viewpoint. Various 1-hydroxyindole derivatives have been prepared from substituted indoles by Somei's method.[2]

Dedicated to the 65th birthday of Prof. Steven M. Weinreb, The Pennsylvania State University.

It has been well-known that tryptophan residues are mainly responsible for near ultraviolet (UV) absorption and fluorescent emission of proteins. Long wavelength absorption band of tryptophans is due to indole moiety with close-lying excited singlet states (S_1 and S_2), and dual fluorescence spectra resulting from $^1L_a \rightarrow {}^1A$ and $^1L_b \rightarrow {}^1A$ fluorescent transitions have been extensively reported[3-9] for indole and related compounds. It has been demonstrated[6] that ^1L_a state is much more sensitive to perturbation of solvent than ^1L_b state. Therefore, fluorescence spectra of tryptophan have been regarded as useful probes for local environment of proteins. Tryptophan-related bioactive compounds examined in the present study are 1-hydroxyindole derivatives such as 1-hydroxy-N_b-methoxycarbonyltryptamine (**1**),[1b] N_b-acetyl-1-hydroxytryptophan methyl ester (**2**),[1b,d] *N*,*N*- dimethyl-1-hydroxyindole-3-acetamide (**3**),[1b] and 1-hydroxy-N_b-pivaloyltryptamine (**4**).[1d]

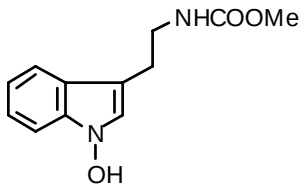

1

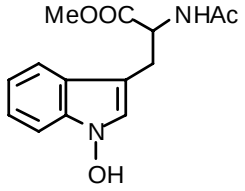

2 (*dl*)

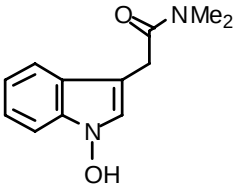

3

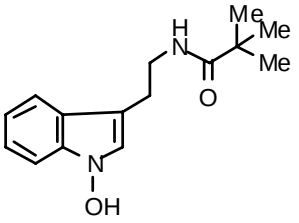

4

For these 1-hydroxyindoles with various C-C-N_b side chains at 3-position of indole ring, it is noticeable whether fluorescence spectra are affected or not by the side chains. Single crystals were fortunately obtained for these 1-hydroxyindoles. Molecular structures taken from X-Ray structure analysis data[1d] of crystalline samples were essential as initial input in molecular orbital calculations. These facts stimulated us to perform geometry optimization of ground state (S_0) in density functional theory (DFT) calculations followed by time-dependent (TD) DFT calculations to estimate energies and oscillator strengths of twenty excited singlet states (S_n).

The present paper describes that 1-hydroxyindoles exhibit dual fluorescence spectra derived from $^1L_a \rightarrow {}^1A$ and $^1L_b \rightarrow {}^1A$ transitions in analogy of those of indole and its derivatives. Fluorescence emission spectrum derived from $^1L_b \rightarrow {}^1A$ transition is more intense than that derived from $^1L_a \rightarrow {}^1A$ for **1** – **3**, and fluorescence emission spectrum derived from $^1L_a \rightarrow {}^1A$ transition is predominant for **4**. It is noteworthy that the perturbation of C-C-N_b side chain induces a significant change in dual fluorescence spectra of 1-hydroxyindoles. On the other hand, 1-hydroxyindoles (**1 – 4)** exhibit almost the same UV absorption spectra consisting of a relatively weak long-wavelength band (λ_{max} = 293, 275 nm). TD-DFT calculations, employed to explain observed electronic spectra, are also described.

EXPERIMENTAL AND COMPUTATIONAL METHODS

Synthesized 1-hydroxyindoles were purified by recrystallization from $CHCl_3$-hexane (for **1** and **3)**, methanol (for **2)**, or AcOEt-hexane (for **4)**. Excellent purities of **1** – **4** were checked by elemental analysis as well as 500 MHz ^{1}H-NMR and mass spectra. Methanol (Kanto Chemical) for HPLC was used without further purification as solvent to prepare sample solution. Absorption spectra were recorded on a Hitachi U-3210 spectrophotometer. Fluorescence excitation and emission spectra of **1** – **4** in air-saturated methanol were measured on a Hitachi F-4500 fluorescence spectrophotometer. Correct fluorescence spectra were calculated

by apparatus coefficients obtained from a calibration with a rhodamine B quantum counter. Relative fluorescence efficiencies were evaluated by weighing printed correct emission spectra on paper. DFT calculations run by Gaussian 03W programs[10] were performed on a work station (Dell Precision 380) with 3.73 GHz Intel Pentium(R) 4 processor extreme edition (2MB L3 cache, 1066MHz FSB). Basis set employed in the DFT calculations for geometry optimization was 6-31G(d) or 6-31G(d,p), and that in the TD-DFT calculations was 6-311+G(d). A three-parameter hybrid density functional, B3LYP,[11] was employed in all the calculations. Polarizable continuum model (PCM) calculations were performed to take methanol into account as solvent. GaussView W 3.0 was used as an affordable, full-featured graphical user interface for Gaussian 03W.

RESULTS AND DISCUSSIONS

I. Possible close-lying ^1L_b and ^1L_a states of 1-hydroxyindole predicted by TD-DFT calculations.

It is believed that indole exhibits dual fluorescence emissions originating from rapidly equilibrated S_1 and S_2. Namely, close-lying fluorescent states (^1L_b and ^1L_a) have been demonstrated to be responsible for the dual fluorescence spectra. Such close-lying ^1L_b and ^1L_a states give rise to the overlapped $^1L_b \leftarrow {}^1A$ and $^1L_a \leftarrow {}^1A$ vibronic absorption bands in the longest absorption spectrum. In comparison with the absorption spectrum of indole in the gas phase, Strickland *et al.*[7] found vibronic peaks with and without shifting to the red in the introduction of methylcyclohexane (C_7H_{13}) as a solvent. The vibronic peaks exhibiting a red-shift were ascribed to the $^1L_a \leftarrow {}^1A$ transition, and those exhibiting almost no shift were ascribed to the $^1L_b \leftarrow {}^1A$ transition. They reported[7] that ^1L_b state locates above ^1L_a state by only 0.12 eV (970 cm^{-1}) in C_7H_{13}, and it was suggested that ^1L_a state becomes S_1 in highly polar solvents.

A complete active space self-consistent field (CASSCF) method and multiconfigurational second-order perturbation theory (CASPT2) calculations of indole were performed by Serrano-Andrés and Roos.[12] The respective energies of ^1L_b and ^1L_a in the gas phase were calculated to be 4.43 and 4.73 eV, which are close to 4.37 and 4.77 eV determined by experiments.[13] In the present study, TD-DFT calculations using B3LYP with 6-311+G(d) basis set were tried for geometry-optimized ground-state of indole in the gas phase. The respective calculated energies of ^1L_b and ^1L_a are 4.85 and 4.71 eV, which are not so different from experimental values and calculated values at CASPT2 level, although the inversion of ^1L_b and ^1L_a in energy is remarkable. It is understood that the inversion is resulted from significant overestimation of ^1L_b. However, TD-DFT calculations are expected to be useful for comparative evaluation of energy and oscillator strength.

Instability of 1-hydroxyindole in solution prevented us to observe its electronic spectra, but TD-DFT calculations were carried out for unstable 1-hydroxyindole as well as indole in methanol. Polarizable continuum model was employed to take account of methanol as a solvent. Molecular orbital (MO) surfaces were drawn at the iso-value of 0.02. No significant difference between indole and 1-hydroxyindole was noticed for surfaces of six MOs (HOMO-2 to LUMO+2). Each MO is more stable in 1-hydroxyindole than in indole. For instance, energies of HOMO and LUMO for 1-hydroxyindole (indole) in methanol were evaluated to be -0.215 (-0.212) and -0.0287 (-0.0241) eV, respectively. A weak perturbation of hydroxy group is thus suggested for electronic spectra.

Table 1 summarizes excitation energies and oscillator strengths of the lowest three excited singlet states (S_1 to S_3) with singly excited configurations for each state. According to CASPT2 calculations[12] of indole, HOMO-1→LUMO and HOMO→LUMO configurations are attributable to primary configurations of ^1L_b and ^1L_a, respectively. Applying the assignments to our TD-DFT calculation results, the respective excitation energies for ^1L_b (S_2) and ^1L_a (S_1) of 1-hydroxyindole (indole) in methanol were estimated to be 4.81 (4.81) and 4.49 (4.58) eV. Dual fluorescence behaviors may be expected for 1-hydroxyindole on the basis of close-lying ^1L_b and ^1L_a, although more elegant calculations should be examined whether ^1L_a locates as S_1 or not.

Table 1. Excitation energies and oscillator strengths of indole and 1-hydroxyindole (1-HI) in methanol obtained by TD-DFT calculations with B3LYP/6-311+G(d).

Compound	Excited States	Excitation Energy			Oscillator Strength, *f*	Singly Excited Configurations [c]
		eV	$\bar{\nu}$ [a] / cm^{-1}	λ [b] / nm		
indole	$S_1(^1L_a)$	4.58	36930	270.8	0.0995	H→L(main); -1→+2, L; -2→L
	$S_2(^1L_b)$	4.81	38790	257.8	0.0367	-1→L & H→+2
	S_3	5.19	41840	239.0	0.0079	H→+1(predominant)
1-HI	$S_1(^1L_a)$	4.49	36230	276.0	0.0955	H→L(main); -1→+2, L
	$S_2(^1L_b)$	4.81	38770	257.9	0.0494	-1→L & H→+2, L
	S_3	5.08	40930	244.3	0.0142	H→+1(predominant)

[a] Wavenumber; [b] Wavelength; [c] H: HOMO, L: LUMO, -N: HOMO-N, +N: LUMO+N

II. Electronic spectra of 1-hydroxyindoles with various C-C-N_b side chains at 3-position in methanol.

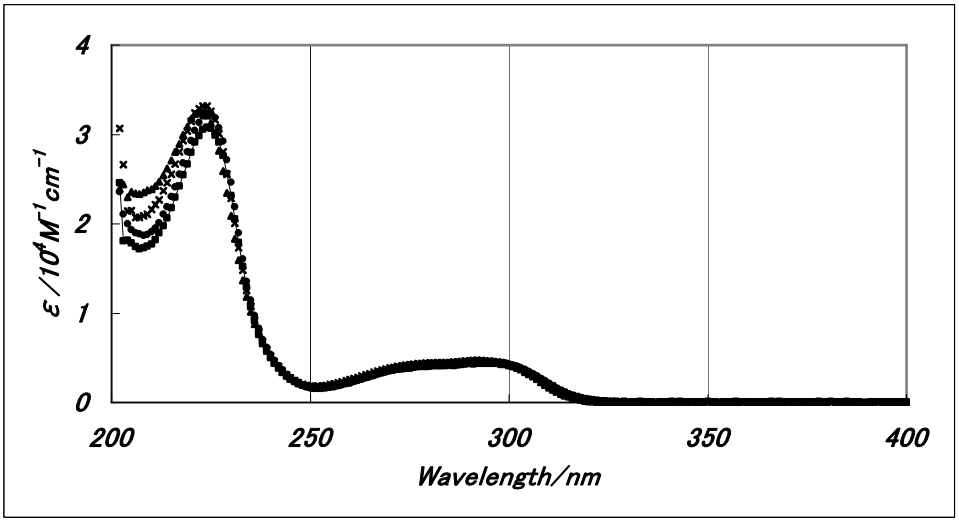

Figure 1. UV absorption spectra of 1-hydroxyindoles (**1** – **4**) with various C-C-N_b side chains at 3-position. Spectrum (■) for **1;** Spectrum (×) for **2**; Spectrum (▲) for **3;** Spectrum (✹) for **4.** Ordinate is molar extinction coefficient.

Almost the same UV absorption spectra were observed for methanol solutions of 1-hydroxyindoles (**1** – **4**)

with various C-C-N_b side chains at 3-position, as shown in Fig. 1. They exhibit a broad spectrum consisting of a relatively weak long-wavelength band (λ_{max} = 292-296 nm) and an intense short-wavelength band (λ_{max} = 222-224 nm). Molar extinction coefficients in $M^{-1}cm^{-1}$ were determined to be 33100 (224 nm) and 4730 (293 nm) for **1**, 33300 (223 nm) and 4710 (292 nm) for **2**, 32600 (222 nm) and 4680 (292 nm) for **3**, and 32400 (224 nm) and 4540 (296 nm) for **4**. Broad spectra of 3-substituted 1-hydroxyindoles in the 250 – 330 nm are different from the reported spectrum of indole,[14] in which a definite peak at 288 nm is accompanied by slightly structured vibronic band in the 250 – 285 nm.

As expected from possible close-lying fluorescent states of 1-hydroxyindole predicted by the aforementioned TD-DFT calculations**,** dual fluorescence spectra were actually observed for 3-substituted 1-hydroxyindoles (**1** – **4**). Methanol solutions of **1** – **4** (0.085 – 0.088 mM) were prepared to exhibit almost the same absorption spectra, and correct fluorescence emission spectra were measured by exciting **1** - **4** at 270 ±5.0 nm. They are collected in Figure 2. Scales of ordinates for the fluorescence spectra of **1** - **4** are not identical.

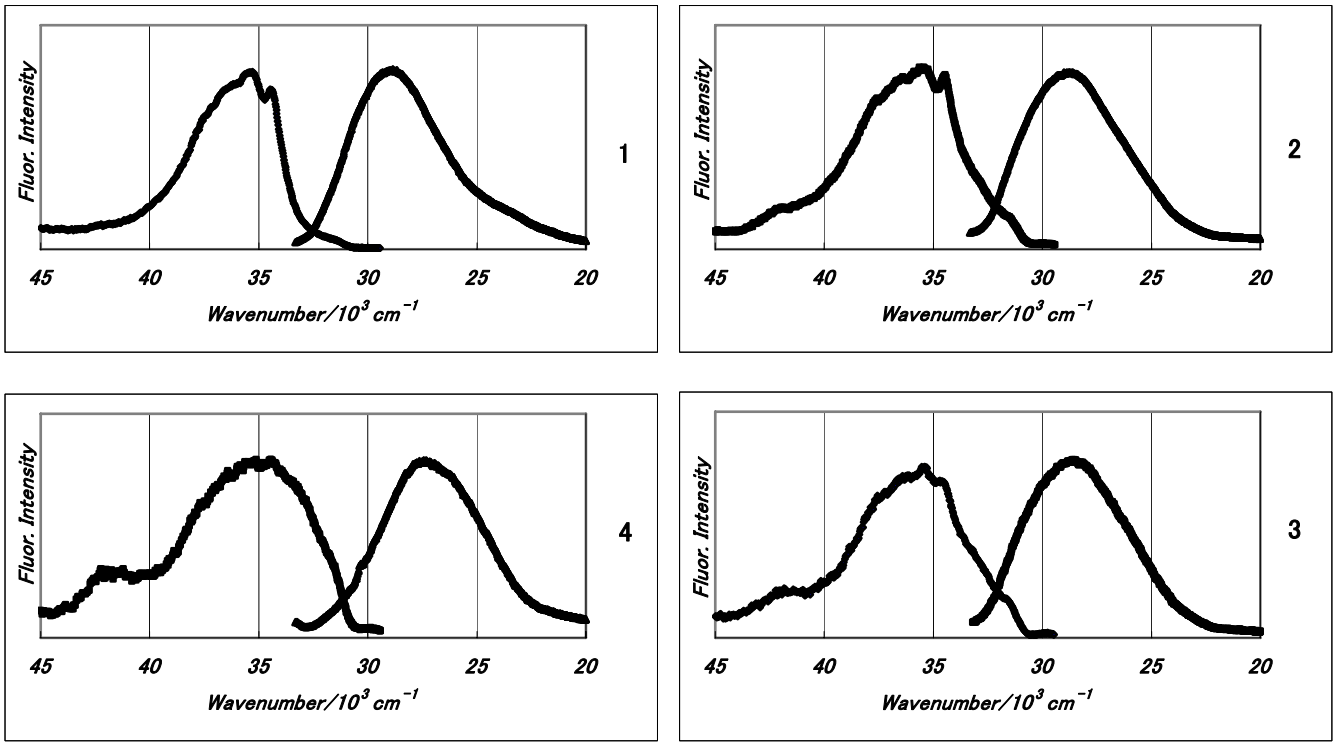

Figure 2. Correct fluorescence excitation and emission spectra of **1** (top left), **2** (top right), **3** (bottom right), and **4** (bottom left) in air-saturated methanol. All emission spectra were observed by exciting of **1** – **4** (0.085 -0.088 mM) at 37040 cm^{-1} (270 nm), and all excitation spectra were observed by monitoring fluorescence emission at the wavenumbers (wavelengths) of maximum intensity. The respective excitation and observation slit widths for emission spectra are 10 and 2.5 nm, and those for excitation spectra are 1.0 and 10 nm. Ordinate is arbitrary fluorescence intensity.

Correct fluorescence emission spectra of **1** – **4** were measured under the same ordinate scale, and the spectra plotted by wavenumber were printed out on paper. The respective relative fluorescence quantum yields of **1**, **2**, **3**, and **4** were determined to be 1.0, 0.30, 0.22, and 0.18 by comparing weights of papers, which were obtained by cutting out spectra. It is noticeable that fluorescence quantum yield is significantly affected by C-C-N_b side chain. Wavenumbers (Wavelengths) at which fluorescence intensity is maximum are 28990 cm^{-1} (345 nm) for **1**, 28770 cm^{-1} (348 nm) for **2**, 28620 cm^{-1} (349 nm) for **3**, and 27310 cm^{-1} (366 nm) for **4**,

respectively. Also shown in Figure 2 are fluorescence excitation spectra, which were obtained by monitoring fluorescence emission at the wavenumbers of maximal fluorescence intensity, mentioned above. It is remarkable that a broad excitation spectrum of **4** is different from those of **1**, **2**, and **3** with some vibrational structures.

Emission spectrum of **1** distinctly exhibits a tail at low energy side. Rapidly equilibrated close-lying fluorescent states imply dual fluorescence emission spectra composed of two slightly shifted fluorescence spectra (A and B). A broad emission spectrum (A) responsible for the tail should be superimposed on a broad emission spectrum (B) in slightly higher energy region. The same situations may be highly probable for both **2** and **3**. Selective observation of lower energy emission spectrum (A) might be attained by monitoring fluorescence at 23260 cm^{-1} (430 nm). On the other hand, observation of higher energy emission spectrum (B) is favorable by monitoring fluorescence at 30300 cm^{-1} (330 nm).

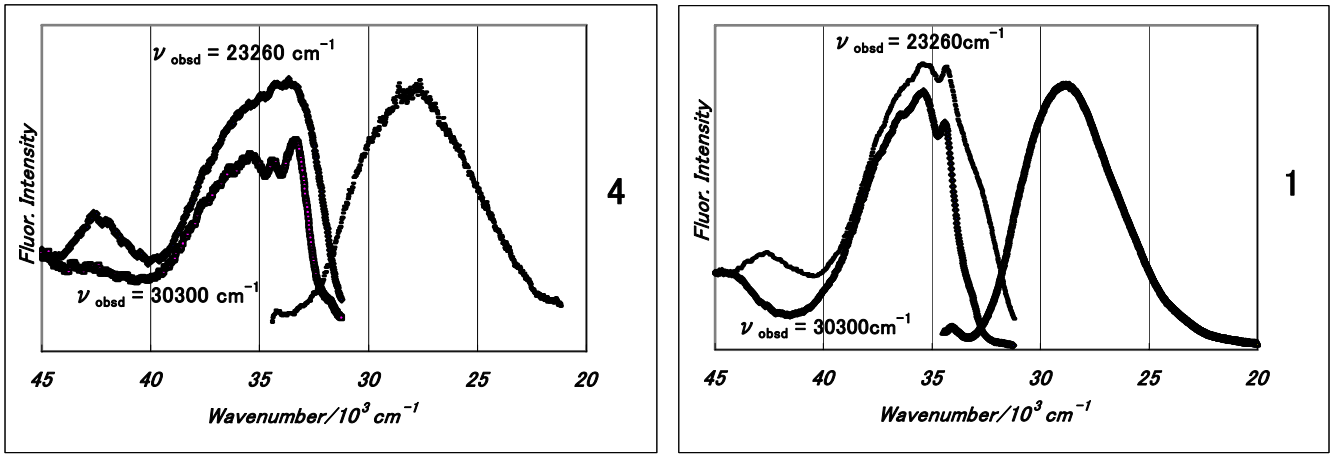

Figure 3. Correct fluorescence excitation and emission spectra of **1** (0.055 mM) and **4** (0.090 mM) in air-saturated methanol. Emission spectra were observed by exciting **1** at 37040 cm^{-1} (270 nm ±2.5 nm) and **4** at 40000 cm^{-1} (250 ±5.0 nm). Slit width for emission is 2.5 nm. Large and small excitation spectra were observed by monitoring fluorescence emission at 23260 cm^{-1} (430 ±5 nm) and 30300 cm^{-1} (330 ±2.5 nm), respectively. Slit width for excitation is 1.0 nm. Ordinate is arbitrary fluorescence intensity.

Figure 3 shows such two kinds of fluorescence excitation spectra for **1** and **4** together with fluorescence emission spectra. Valeur and Weber[9] reported the resolution of fluorescence excitation spectrum of tryptophan in propylene glycol at -58 °C into the ^1L_a and ^1L_b excitation bands. A broad excitation spectrum of **4** observed at 23260 cm^{-1} (430 nm) is very similar to the ^1L_a excitation band of tryptophan, and a slightly structured excitation spectra observed at 30300 cm^{-1} (330 nm) is similar to the ^1L_b excitation band of tryptophan. Drastic change in the excitation spectra clearly supports dual fluorescence emission spectra consisting of $^1L_a \rightarrow {}^1A$ and $^1L_b \rightarrow {}^1A$ fluorescence emission spectra (A and B), and selective observation of A is achieved at 23260 cm^{-1}. The lowest energy peak at 33310 cm^{-1} (4.13 eV) can be regarded as the 0,0-band of ^1L_b excitation spectrum.

With respect to **1**, both excitation spectra observed at 23260 and 30300 cm^{-1} exhibit similar vibronic structure. This indicates that both A and B are observed at 23260 cm^{-1} in contrast to the selective observation of A for **4**. Taking the lowest energy peak as 0,0-band of ^1L_b excitation spectrum, the energy of ^1L_b was determined to be 34410 cm^{-1} (4.27 eV). It is noteworthy that a swelling is seen at low energy edge in the excitation spectrum observed at 23260 cm^{-1}. The fact strongly implies that a broad ^1L_a excitation band is superimposed on a

structured ^1L_b excitation band. Namely, the band origin of ^1L_a should be placed in the swelling. It is thus confirmed that ^1L_a state is S_1. Similar dual fluorescence excitation spectra were observed for **2** and **3**.

Dual fluorescence excitation and emission spectra were demonstrated for 3-substituted 1-hydroxyindoles (**1** – **4**). It is concluded that $^1L_b \rightarrow {}^1A$ fluorescence emission is mainly responsible for the observed dual emission spectra of **1**, **2**, and **3**, and that $^1L_a \rightarrow {}^1A$ fluorescence emission is mainly responsible for that of **4**. It is noteworthy that dual fluorescence spectra are delicately affected by C-C-N_b side chain at 3-position of indole ring. The energies of ^1L_b were determined to be 34410 cm^{-1} (4.27 eV) for **1**, 34460 cm^{-1} (4.27 eV) for **2** and 34700 cm^{-1} (4.30 eV) for **3**, and 33310 cm^{-1} (4.13 eV) for **4**, respectively. ^1L_a should be S_1 for **1** – **4**.

III. TD-DFT calculations of 1-hydroxyindoles with various C-C-N_b side chains at 3-position in methanol.

Table 2. Excitation energies and oscillator strengths (*f*) of 3-substituted 1-hydroxyindoles in methanol obtained by TD-DFT calculations with B3LYP/6-311+G(d). Excitation energies and molar extinction coefficients (ε) of observed absorption peaks are shown by bald letters.

1-HIs	Excited States	Excitation Energy			*f*	Singly Excited Configurations[c]
		eV	$\bar{\nu}$ [a] / cm^{-1}	λ [b] / nm	$\varepsilon / M^{-1}cm^{-1}$	
1		**4.232**	**34130**	**293.0**	**4730**	
	$S_1(^1L_a)$	4.331	34930	286.3	0.0981	H→L(main) & -1→+3
	$S_2(^1L_b)$	4.750	38310	261.0	0.0253	-1→L(main); H→+3, +2, +1
	S_3	4.904	39560	252.8	0.0130	H→+1(main) & H→+2
	S_4	5.308	42810	233.6	0.0300	H→+2(main); H→+3, +1, +5
2		**4.246**	**34250**	**292.0**	**4710**	
	$S_1(^1L_a)$	4.374	35270	283.5	0.0823	H→L(main); -1→+3, L
	S_2	4.518	36440	274.4	0.0139	H→+1(predominant)
	$S_3(^1L_b)$	4.773	38490	259.8	0.0439	-1→L(main); H→+3, +4, +2
	S_4	4.919	39680	252.0	0.0129	H→+2(main); H→+3, +4
3		**4.243**	**34220**	**292.2**	**4680**	
	$S_1(^1L_a)$	4.343	35030	285.5	0.0867	H→L(predominant)
	$S_2(^1L_b)$	4.742	38240	261.5	0.0236	-1→L(main); H→+3, +2, +1
	S_3	4.906	39570	252.7	0.0159	H→+1(main) & H→+4
	S_4	5.075	40930	244.3	0.0604	H→+2(main) & H→+3
4		**4.188**	**33780**	**296.0**	**4540**	
	$S_1(^1L_a)$	4.325	34880	286.7	0.1025	H→L(predominant)
	$S_2(^1L_b)$	4.749	38300	261.1	0.0245	-1→L(main); H→+2, +3, +4, +1
	S_3	4.884	39390	253.9	0.0145	H→+1(main); H→+2, +3; -1→L
	S_4	5.240	42270	236.6	0.0360	H→+2(main); H→+1, +3, +6

[a] Wavenumber; [b] Wavelength; [c] H: HOMO, L: LUMO, -N: HOMO-N, +N: LUMO+N

Geometry optimizations of 3-substituted 1-hydroxyindoles (**1** – **4**) in the ground state were carried out by DFT calculation using B3LYP functional with 6-31G(d,p) basis set. Initial parameters (bond distance, bond angle, and dihedral angle) of molecular structure were taken from X-Ray structure analysis data of crystalline samples. Angles between N-OH bond and indole ring in **1** – **4** were obtained to be 12.2, 15.2, 10.9, and 2.3 degree, respectively. Putting dummy atom (X) at the center of gravity of five-membered pyrrole ring, the respective X-N-O bond angles of **1** – **4** were calculated to be 13.5, 8.0, 7.5, and 3.5 degree by DFT geometry optimization in the gas phase. Such small deviations of N-OH bond from indole plane predicted both by X-Ray structure analysis and by DFT calculation are comparable with each other except for those of **2**, and they should be intrinsic of 1-hydroxyindoles with C-C-N_b side chain. Noticeable are that N-hydroxy groups of **1**, **2**, and **3** are not in the plane of indole ring, and that of **4** is nearly in the plane. Such a difference is important to determine reaction pathways on chemical reactions of **1** – **4** with 85% formic acid. Namely, compounds **1** – **3** undergo regioselective nucleophilic substitution reaction providing serotonine derivatives, while **4** undergoes dimerization.[1]

TD-DFT calculations of geometry-optimized 3-substituted 1-hydroxyindoles (**1** – **4**) were performed by using B3LYP functional with 6-311+G(d) basis set. Table 2 summarizes calculated excitation energies and oscillator strengths of S_1 – S_4 with singly excited configurations. Notations of ^1L_b and ^1L_a are employed, although indole symmetry is perfectly lost by C-C-N_b side chain. ^1L_a state is S_1 for **1** – **4**, while ^1L_b state is S_2 for **1**, **3**, and **4**, and S_3 for **2**. It has been demonstrated that substitution on pyrrole ring affects ^1L_a state qualified as ethylene-like in nature, and that substitution on benzenoid ring affects ^1L_b state qualified as benzene-like in nature. Electron densities of LUMO+1 MO of **2** localize on C-C-N_b side chain. This is not the case for LUMO+1 MOs of **1**, **3**, and **4**. It is reasonable that the excited singlet state deriving mainly from HOMO→LUMO+1 singly excited configuration is greatly stabilized by the C-C-N_b side chain.

Judging from oscillator strengths, both ^1L_a and ^1L_b excited states deriving mainly from HOMO→LUMO and HOMO-1→LUMO singly excited configurations are essentially responsible for UV absorption spectra of 1-hydroxyindoles. Additional two excited singlet states deriving mainly from HOMO→LUMO+1 and HOMO→LUMO+2 configurations are also responsible for those of 1-hydroxyindoles. UV absorption spectra with a peak at 292-294 nm and a shoulder peak at 275 nm may appear through the superposition of S_1←S_0, S_2←S_0, S_3←S_0, and S_4←S_0 absorption bands broadened by strong solute-solvent interaction. Similar absorption spectra of **1**, **3**, and **4** are consistent with almost the same excitation energies and oscillator strengths. Observed UV absorption spectrum of **2** is also similar to those of **1**, **3**, and **4** in spite of considerable oscillator strength (0.0439) for ^1L_b (S_3) of **2**.

Dual fluorescence behaviors of 3-substituted 1-hydroxyindoles (**1** – **4**) should be examined by TD-DFT calculations. Dual fluorescence excitation spectra consist of a broad ^1L_a excitation band at lower energy side and a slightly structured ^1L_b excitation band at higher energy side, and ^1L_a and ^1L_b states are close-lying. Observed (calculated) energies of ^1L_b states are 4.27 (4.75) eV for **1**, 4.27 (4.77) eV for **2**, 4.30 (4.74) eV for **3**, and 4.13 (4.75) eV for **4**, respectively. TD-DFT calculations result in an overestimation. The assignment of ^1L_a as S_1 in TD-DFT calculations is consistent with experimental results. However, an overestimation of ^1L_a

is also confirmed in TD-DFT calculations. Calculated oscillator strength (0.1025) of ^1L_a (S_1) and the energy gap (0.424 eV) between ^1L_a (S_1) and ^1L_b (S_2) for **4** are the largest of all. The facts are consistent with main contribution of $^1L_a \rightarrow {}^1A$ fluorescence for dual fluorescence emission spectra of **4**. However, considerably different dual fluorescence behaviors of **1** and **4** cannot be explained by almost the same energies and oscillator strengths of $S_1 - S_4$. More sophisticated calculations such as CASSCF/PT2 are expected to discuss the effect of C-C-N_b side chain on dual fluorescence behaviors.

CONCLUSIONS

Dual fluorescence excitation and emission spectra resulting from close-lying ^1L_a and ^1L_b states were observed for 1-hydroxyindoles (**1** – **4**) in methanol at room temperature. As is distinct from almost the same UV absorption spectra, dual fluorescence spectra are somewhat different from each other. The lowest excited singlet state (S_1) was assigned to ^1L_a, because ^1L_a excitation spectrum was obtained by a selective observation of $^1L_a \rightarrow {}^1A$ fluorescence at low energy tail of dual fluorescence emission spectra. Consequently, ^1L_b state locates above ^1L_a state. The assignment was supported by TD-DFT calculations.

Fluorescence quantum yield is significantly affected by C-C-N_b side chain. The highest and the lowest values are given to **1** and **4**, respectively. $^1L_b \rightarrow {}^1A$ fluorescent transition with less oscillator strength is mainly responsible for the fluorescence emission spectra of **1**, while $^1L_a \rightarrow {}^1A$ fluorescent transition with larger oscillator strength is mainly responsible for the fluorescence emission spectra of **4**. Assuming that larger oscillator strength gives rise to higher fluorescence quantum yield, these facts contradict with each other. It is therefore implied that non-radiative transition competing with $^1L_a \rightarrow {}^1A$ fluorescent transition is much more effective than that competing with $^1L_b \rightarrow {}^1A$ fluorescent transition. It is noteworthy that changes in energies and oscillator strengths of ^1L_a and ^1L_b states may be caused by C-C-N_b side chain at 3-position of indole ring, and it is recognized that dual fluorescence spectra exhibit a significant response against such changes. Significant response of dual fluorescence behaviors demonstrates that various bioactive 1-hydroxytryptophanes and related compounds should be a probe of local environment in proteins.

ACKNOWLEDGEMENTS

The authors are indebted to Prof. Fumio Yamada for X-Ray structure analysis. We also wish to thank Dr. Tomonori Ida (Kanazawa University) for helpful comments and discussions on density functional theory calculations.

REFERENCES

1. a) M. Somei, *J. Synth. Org. Chem.*, 1991, **49**, 205; b) M. Somei, *Heterocycles*, 1999, **50**, 1157; c) M. Somei, Advances in Heterocyclic Chemistry, Vol. 82, ed. By A. R. Katritzky, Elsevier Science, USA, 2002, pp. 101-155.; d) M. Somei, Topics in Heterocyclic Chemistry, Vol. 6, ed. By S. Eguchi, Springer-Verlag, Berlin, 2006, pp. 77-111.

2. M. Somei and T. Kawasaki, *Heterocycles*, 1989, **29**, 1251; M. Somei, T. Kawasaki, K. Shimizu, Y. Fukui, and T. Ohta, *Chem. Pharm. Bull*., 1991, **39**, 1905.
3. G. Weber, *Biochem. J.*, 1960, **75**, 335.
4. H. Zimmerman and N. Joop, *Z. Elektrochem*., 1961, **65**, 61.
5. P. –S. Song and W. E. Kurtin, *J. Am. Chem. Soc.*, 1969, **91**, 4892.
6. E. H. Strickland, J. Horwitz, and C. Billups, *Biochem*., 1970, **9**, 4914.
7. E. H. Strickland, C. Billups, and E. Kay, *Biochem*., 1972, **11**, 3657.
8. A. Andrews and L. S. Forster, *Photochem. Photobiol.*, 1974, **19**, 353.
9. B. Valeur and G. Weber, *Photochem. Photobiol.*, 1977, **25**, 441.
10. Gaussian 03, Revision C.02, M. J. Frisch, G. W. Trucks, H. B. Schlegel, G. E. Scuseria, M. A. Robb, J. R. Cheeseman, J. A. Montgomery, Jr., T. Vreven, K. N. Kudin, J. C. Burant, J. M. Millam, S. S. Iyengar, J. Tomasi, V. Barone, B. Mennucci, M. Cossi, G. Scalmani, N. Rega, G. A. Petersson, H. Nakatsuji, M. Hada, M. Ehara, K. Toyota, R. Fukuda, J. Hasegawa, M. Ishida, T. Nakajima, Y. Honda, O. Kitao, H. Nakai, M. Klene, X. Li, J. E. Knox, H. P. Hratchian, J. B. Cross, C. Adamo, J. Jaramillo, R. Gomperts, R. E. Stratmann, O. Yazyev, A. J. Austin, R. Cammi, C. Pomelli, J. W. Ochterski, P. Y. Ayala, K. Morokuma, G. A. Voth, P. Salvador, J. J. Dannenberg, V. G. Zakrzewski, S. Dapprich, A. D. Daniels, M. C. Strain, O. Farkas, D. K. Malick, A. D. Rabuck, K. Raghavachari, J. B. Foresman, J. V. Ortiz, Q. Cui, A. G. Baboul, S. Clifford, J. Cioslowski, B. B. Stefanov, G. Liu, A. Liashenko, P. Piskorz, I. Komaromi, R. L. Martin, D. J. Fox, T. Keith, M. A. Al-Laham, C. Y. Peng, A. Nanayakkara, M. Challacombe, P. M. W. Gill, B. Johnson, W. Chen, M. W. Wong, C. Gonzalez, and J. A. Pople, Gaussian, Inc., Wallingford CT, 2004.
11. A. D. Becke, *J. Chem. Phys*. 1993, **98**, 5648.
12. L. Serrano-Andrés and B. O. Roos, *J. Am. Chem. Soc.*, 1996, **118**, 185.
13. P. Ilich, Can. *J. Spectrosc*. 1987, **67**, 3274.
14. D. C. Merrer, S. Ozcetinkaya, and A. E. Shinnar, *Tetrahedron Lett.*, 2004, **45**, 4899.